International Journal of Solids and Structures 47 (2010) 716–729

Contents lists available at ScienceDirect

International Journal of Solids and Structures

journal homepage: www.elsevier.com/locate/ijsolstr

Homogenization of elasto-plastic composites coupled with a nonlinear finite element analysis of the equivalent inclusion problem

L. Brassart *, I. Doghri, L. Delannay

Université catholique de Louvain, Department of Mechanical Engineering, 4 Av. Georges Lemaître, B-1348 Louvain-la-Neuve, Belgium

ARTICLE INFO

Article history:
Received 27 August 2009
Received in revised form 19 October 2009
Available online 26 November 2009

Keywords:
Composite materials
Homogenization
Elasto-plasticity
Finite element
Mean-field
Incremental
Mori-Tanaka
Isolated inclusion

ABSTRACT

This paper deals with the micromechanical modeling of particle reinforced elasto-plastic composites under general non-monotonic loading histories. Incremental mean-field (MF) homogenization models offer an excellent cost-effective solution, however there are cases where their predictions are inaccurate. Here, we assess the applicability of the equivalent inclusion representation, which sustains many homogenization schemes. To this end, MF models are fully coupled with a finite element (FE) solution of the equivalent inclusion problem (EIP). Consequently, Eshelby's tensor is not used and most (but not all) approximations involved in the generalization of MF models from linear elasticity to the nonlinear regime are avoided. The proposal is implemented for Mori-Tanaka (M-T) and dilute inclusion models and applied to several composite systems with elasto-plastic matrix and spherical or ellipsoidal particles, subjected to various loadings (tension, plane strain, cyclic tension/compression). The predictions are verified against reference full-field FE simulations of multiparticle cells. Results show that the M-T model coupled with the nonlinear FE solution of the EIP is very accurate at the macro level up to 25% volume fraction of reinforcement, while the phase averages remain accurate as long as the volume fraction does not exceed 15%. The strain concentration tensor computed almost exactly from single inclusion FE analysis is compared against approximate expressions assumed by classical MF models. Implications for the development of advanced MF homogenization models are discussed.

1. Introduction

Linking the mechanical response of particle-reinforced elastic–plastic composites to the underlying microstructure is relevant in a variety of technological applications. One example is the design and the optimization of the forming operations of multiphase metallic alloys. When constitutive phases have contrasted strengths, both the anisotropic plastic flow and the hardening (especially the kinematic hardening component which dictates elastic springback) depend on the volume fraction, the size, the shape and the topological distribution of the reinforcing phase(s) (e.g. Corbin et al., 1996; Guillemer-Neel et al., 1999; Delannay et al., 2009).

Accurate predictions of the effective response of such composite materials may be derived from full-field calculation of the local stresses and strains throughout a statistically representative volume element (RVE) of the microstructure subjected to periodic boundary conditions. For instance, Segurado et al. (2002) and Pierard et al. (2007) considered respectively spherical and ellipsoidal inclusions randomly distributed in a continuous matrix, and solved the boundary value problem with the finite element (FE) method. In supplement to the overall mechanical response, the local fields may be used to predict the onset of damage (Han et al., 2001; LLorca and Segurado, 2004; Segurado and LLorca, 2006). Such modeling is however too costly when applied to the simulation of real-scale structures made of composite materials.

Alternatively, when one seeks only the homogenized response of the composite, mean-field (MF) approaches can efficiently be relied upon. Their remarkably low computational cost – as compared to full-field computation over a RVE – allows them to be used as implicit constitutive laws in large scale simulations. For particle-reinforced, linear elastic materials, MF approaches are usually based on the companion problem of a single inclusion embedded in an infinite, reference medium. Interactions among inclusions are accounted for, in a simplified way, through the mechanical behavior assigned to the reference medium or through the definition of the far-field strain. For instance, the well-known Mori-Tanaka model (M-T) (Mori and Tanaka, 1973) assumes that the single inclusion is embedded in the matrix material and sees the matrix average strain as far-field strain (Benveniste, 1987). In the self-consistent scheme (Hershey, 1954; Kröner, 1958), the reference medium bears the effective properties of the composite and

* Corresponding author.
E-mail addresses: laurence.brassart@uclouvain.be (L. Brassart), issam.doghri@uclouvain.be (I. Doghri), laurent.delannay@uclouvain.be (L. Delannay).

0020-7683/$ - see front matter © 2009 Elsevier Ltd. All rights reserved.
doi:10.1016/j.ijsolstr.2009.11.013

the system is subjected to the real macroscopic strain. The (semi-) analytical solution of this "Equivalent Inclusion Problem" (EIP) is based on the seminal work of Eshelby (1957). Strain localization tensors relating the phase averages of the strain field to the macroscopic strain are then available in closed form.

When the composite constituents have nonlinear behavior, additional assumptions are introduced in MF homogenization schemes. For instance, one usually relies on the concept of Linear Comparison Composite (LCC). In secant methods (Berveiller and Zaoui, 1979; Tandon and Weng, 1988; Suquet, 1995), the phases of the LCC are defined by the secant moduli of the actual phases, computed at a well-chosen, reference strain or stress. More sophisticated definitions of LCC's were proposed by Ponte Castañeda (1996, 2002) for instance, based on variational formulations. These methods apply to elasto-plastic behavior within the framework of the deformation theory of plasticity, which precludes their use in non-monotonic loading conditions.

The work-around for dealing with general loading histories is provided by incremental approaches, initially proposed by Hill (1965) for the self-consistent modelling of polycrystals. Constitutive equations of rate-independent materials are written in rate form $\dot{\boldsymbol{\sigma}} = \boldsymbol{C} : \dot{\boldsymbol{\varepsilon}}$ and linearized over each time interval. For rate-dependent materials, in the affine formulation due to Masson and Zaoui (1999), and enhanced by Pierard and Doghri (2006a), thermoelastic comparison materials are defined from tangent operators of the phases. As the tangent operator $\boldsymbol{C}$ of an elastic-(visco)plastic material depends on the strain history, it is not uniform throughout each phase of the EIP. Applying Eshelby's reasoning hence requires the definition of comparison materials having uniform tangent moduli. It is long known that making use of the algorithmic tangent operator computed for the average strain and strain increment of the phase gives a too stiff response (Gilormini, 1995). Better predictions are obtained when one computes the isotropic part of the algorithmic tangent operator according to a spectral decomposition due to Ponte Castañeda (1996). However, the theoretical justification is not totally clear (Chaboche et al., 2005; Pierard and Doghri, 2006b). Doghri and Ouaar (2003) used this isotropic approximation together with a Mori-Tanaka scheme to simulate the behavior of elasto-plastic composites under cyclic loading. When applied to dual-phase steel, the model correctly captures the macroscopic response, but tends to underestimate the inclusion stress level (Delannay et al., 2007).

The above-mentioned models mainly focus on the definition of the linear comparison materials, while little attention is paid to the localization problem, which is tackled within the framework of linear elasticity using available homogenization schemes for linear composites. However, the definition of the LCC and the choice of the linear homogenization scheme both influence the prediction of the effective response of the nonlinear composite. Due to the coupling between these two modeling assumptions, it is difficult to assess each one of them separately. Recently, Rekik et al. (2007) proposed a methodology for comparing several LCC's proposed in the literature, circumventing approximations related to the homogenization of the LCC by a linear MF homogenization scheme. To this end, the homogenization problem associated with the LCC is solved by the FE method, considering identical microstructures for the actual nonlinear composite and the LCC. Local fields in the LCC are then identified to the actual ones in the nonlinear composite. In order to reduce the computational cost, the authors considered a very simple microstructure (although the methodology is not restricted to this particular case), consisting of a hexagonal array of inclusions. Considering axially symmetric loading conditions, this periodic microstructure could be modelled by a 2D axisymmetric cell containing a single inclusion.

The present work focuses on the applicability to nonlinear composites of the equivalent inclusion representation, that is, a single inclusion with *infinitesimal* volume fraction. Here, the EIP is solved "exactly" (in the FE sense) considering the actual *nonlinear* behavior of the surrounding matrix. Therefore, Eshelby's solution is neither needed nor used. In this way, the relevance of the EIP for representing nonlinear composites may be assessed separately from the choice of a LCC. Phase interactions are accounted for within the framework of an extended Mori-Tanaka scheme. According to the interpretation of this scheme due to Benveniste (1987), the EIP is solved considering the (a priori unknown) matrix average strain as far-field strain. The M-T model is coupled with the FE solution of the EIP through an iterative procedure, and the ability to capture phase interactions by an isolated inclusion model is discussed. This methodology was initially proposed by Brassart et al. (2009) for hyperelastic composites subjected to interface decohesion under hydrostatic loading conditions.

The new proposal is applied to two-phase composites made of an elasto-plastic matrix reinforced by linear elastic inclusions. Random arrangements of spherical and aligned, ellipsoidal inclusions with identical shapes are successively considered. More general inclusions arrangements are not considered in this study, as it is well-known that the M-T model may lead to unphysical results when the inclusions have different aspect ratios and orientations (Qiu and Weng, 1990; Benveniste et al., 1991). The validity of the scheme is studied under cyclic loadings and for several volume fractions of inclusions, by comparing the predictions of the MF model to reference results obtained by the FE method on representative unit cells containing about thirty randomly dispersed inclusions. We particularly focus on the predictive capabilities of the M-T model of the inclusion response. Additionally, the FE solution of the EIP is used to compute a strain concentration tensor by a pertubation method. This "exact" strain concentration tensor is compared to semi-analytical expressions used in the incremental MF models of Pierard and Doghri (2006b) and Delannay et al. (2007).

This paper is organized as follows. First, the generation of representative unit cells providing reference predictions of the composite response and the reference solution of the EIP is presented in Section 2. Section 3 is devoted to the MF homogenization model based on a FE solution of the single inclusion problem. The predictions are compared to the reference results in Section 4. Approximate solutions of the EIP provided by MF models are discussed in Section 5 by comparing their strain concentration tensors to a reference one computed by a perturbation method. Finally, results of Sections 4 and 5 are discussed in view of their implications for further improvements of MF schemes, before concluding.

Throughout the paper, Einstein's convention is used, with indices ranging from 1 to 3, unless otherwise indicated. The different products are expressed as $(\boldsymbol{A} : \boldsymbol{\sigma})_{ij} = A_{ijkl}\sigma_{lk}$, $\boldsymbol{A} :: \boldsymbol{B} = A_{ijkl}B_{lkji}$, and $(\boldsymbol{\sigma} \otimes \boldsymbol{\sigma})_{ijkl} = \sigma_{ij}\sigma_{kl}$. The symbols $\boldsymbol{1}$ and $\mathbf{I}$ stand for the second and symmetric fourth-order identity tensors, respectively. Finally, the spherical and deviatoric operators $\boldsymbol{I}^{\mathrm{vo}}$ and $\boldsymbol{I}^{\mathrm{dev}}$ are given by:

$$\boldsymbol{I}^{\mathrm{vol}} \equiv \frac{1}{3}\boldsymbol{1} \otimes \boldsymbol{1}, \quad \boldsymbol{I}^{\mathrm{dev}} \equiv \boldsymbol{I} - \boldsymbol{I}^{\mathrm{vol}}. \tag{1}$$

2. Model microstructures and FE simulations

The idealized microstructure considered in this study consists of a random arrangement of spherical or ellipsoidal inclusions embedded in a continuous matrix. The volume fraction of inclusions is varied from 5% to 35% and the micro-macro transition schemes are evaluated in every case. When the volume fraction is very low, the mechanical response of the composite may be captured by considering a single, isolated inclusion. However, when the volume fraction increases, nearby inclusions start to interact and this affects the overall mechanical behavior. Simulations must

then be performed on a Representative Volume Element (RVE) of the microstructure. The number of inclusions is considered statistically representative if the composite response is unchanged when the number of inclusions is raised further at constant volume fraction. Here, this number is set equal to 30, as already recommended by Segurado et al. (2002) for an elasto-plastic composite reinforced by spherical inclusions. Indeed, the scatter of the macroscopic response for several distributions of 30 inclusions is lower than 5%. Similarly, Pierard et al. (2007) have shown that dispersions of 30 aligned ellipsoidal inclusions form statistically homogeneous and transversely isotropic composite cells.

The generation of the random distribution follows (Pierard et al., 2007). Rectangular prisms of dimensions $\alpha L \times L \times L$ are filled with identical and aligned ellipsoids whose longitudinal and transverse semi-axes are αr and r, respectively. The RVE microstructure is periodic along the 3 directions, allowing us to apply periodic boundary conditions to the prism faces. In this way, the effective response of the composite is closer to that of an infinite RVE than that obtained under imposed force or displacement (Hazanov and Huet, 1994). The inclusion positioning is constrained by the practical limitation of generating an acceptable FE mesh. Therefore, the minimal distance between the surfaces of two ellipsoids has to be larger than $0.035\alpha r$. This also prevents some clustering effects, as the average stress within an inclusion is influenced by the minimal distance between inclusions (Weissenbek et al., 1994; Delannay et al., 2007; Segurado and LLorca, 2006). A similar criterion applies to the minimal distance between each ellipsoid surface and the prism faces, edges or corners, which must be larger than $0.05\alpha r$.

The representative cells are meshed using NETGEN (2004) with quadratic tetrahedra. A typical mesh comprises about 160,000 elements and 220,000 nodes. FE simulations are performed using ABAQUS (2007) and the whole volume is meshed using 10-node tetrahedra (C3D10M in ABAQUS), which have three extra internal degrees of freedom compared with standard 10-noded tetrahedra, enabling us to better capture the strain gradients in the matrix. Convergence study was successfully conducted by comparing the predictions (effective response and average inclusion response) to those obtained with finer meshes (about 200,000 elements). Fig. 1(a) and (b) show typical meshes for a composite with 15% of spherical or ellipsoidal inclusions.

The macroscopic stress predicted by the FE analysis is computed from a volume average of the stress tensor given at each integration point over the RVE of domain ω:

$$\bar{\boldsymbol{\sigma}} \equiv \frac{1}{V(\omega)} \sum_{k=1}^{N_k} \boldsymbol{\sigma}_k V_k, \tag{2}$$

where $\boldsymbol{\sigma}_k$ is the stress at the integration point k, V_k is the volume associated with the integration point k and $V(\omega)$ is the total volume of the RVE. The same method applies for computing the average of stress and strain fields over the inclusion or matrix domains. The stress–strain curves presented in the following were obtained by averaging 3 simulations over cells with statistically equivalent topologies.

The modeling strategy presented in the next section relies on a FE solution of the EIP in elasto-plasticity. This solution is obtained

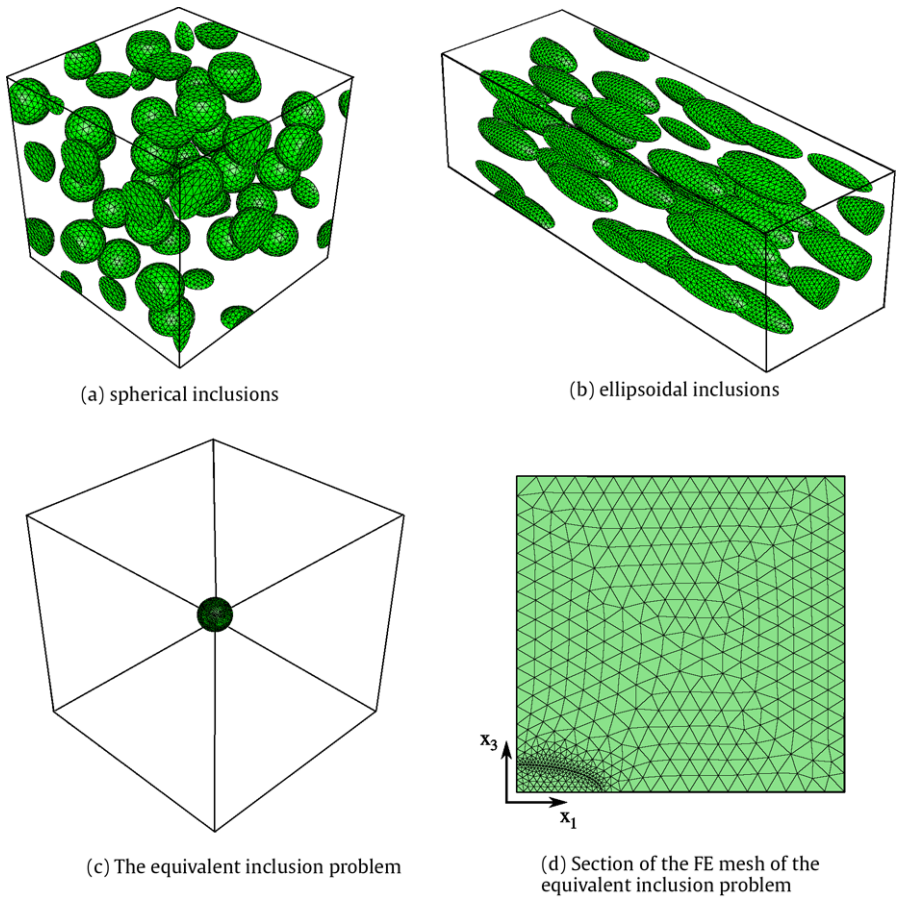

Fig. 1. Multiparticle vs. single particle modeling of composites. Multiparticle modeling of composite is performed by FE computation on representative cells comprising 30 spherical (a) or ellipsoidal ($\alpha = 3$) (b) inclusions in a continuous matrix, with volume fractions ranging from 5% to 35%. Alternatively, an isolated inclusion modeling is considered, in which the volume fraction is 0.1% (c). When symmetry conditions hold, the FE computation is performed on one eight of the single inclusion cell (d).

by solving the boundary value problem on a cubic unit cell of length L containing a single inclusion placed at its center (Fig. 1(c)). In the EIP, the volume fraction of inclusion is infinitesimal. In practice, the relative difference on the particle strain obtained with cells containing respectively 1% and 0.1% volume fraction of inclusion was close to 1% for the two-phase steel considered in this paper. Therefore, it is assumed that setting the volume fraction of the single inclusion to 0.1% is an acceptable approximation of the dilute inclusion problem. Displacement boundary conditions are applied as:

$$\boldsymbol{u}(\boldsymbol{x}) = \boldsymbol{\varepsilon}^{\infty} \cdot \boldsymbol{x} \quad \forall \boldsymbol{x} \in \partial\omega^*, \tag{3}$$

where ω^* is the domain of the isolated inclusion cell and $\boldsymbol{\varepsilon}^{\infty}$ is the far-field strain.

When the principal loading axes are aligned with the ellipsoid semi-axes, and considering isotropic response of the inclusion and the matrix, symmetry allows us to reduce the problem size by meshing only one eight of the EIP. The particle is placed at the corner (0, 0, 0) of the cell, the ellipsoid semi-axes being aligned with the symmetry directions (see Fig. 1(d)). Displacement boundary condition (3) becomes:

$$\begin{cases} u_1(0,x_2,x_3) = 0 \\ u_2(x_1,0,x_3) = 0 \quad 0 \leqslant x_1,x_2,x_3 \leqslant L \\ u_3(x_1,x_2,0) = 0 \\ u_i(\boldsymbol{x}) = \varepsilon^{\infty}_{ij} x_j \qquad x_1 = L, x_2 = L \text{ or } x_3 = L \end{cases} \tag{4}$$

The discretization of the reduced unit cell comprises approximately 16,000 elements and 26,000 nodes, while the fully discretized cell comprises about 40,000 elements and 60,000 nodes. In both cases, convergence of the simulations was assessed by comparing the results with those obtained with finer meshes. Again, the FE simulations are performed with ABAQUS (2007), and the whole volume (matrix and inclusion) is meshed with modified 10-node tetrahedra (C3D10M in ABAQUS, 2007).

3. Homogenization based on the finite element solution of the equivalent inclusion problem

3.1. Methodology

In this section, a methodology is proposed to assess the relevance of the single inclusion modeling of elasto-plastic composites. The Mori-Tanaka scheme, as interpreted by Benveniste (1987), is coupled to a FE resolution of the equivalent inclusion problem. Therefore, approximations related to the definition of a reference material for the nonlinear matrix are (to a large extent) circumvented and Eshelby's solution is neither needed nor used.

Consider a representative volume element (RVE) of a two-phase, nonlinear composite subjected to a given macroscopic strain $\bar{\boldsymbol{\varepsilon}}$. In a mean-field approach, we aim to compute the strain partitioning between the matrix (domain ω_0) and the inclusions (domain ω_1), so that:

$$\bar{\boldsymbol{\varepsilon}} = c_0 \langle \boldsymbol{\varepsilon} \rangle_{\omega_0} + c_1 \langle \boldsymbol{\varepsilon} \rangle_{\omega_1}, \tag{5}$$

where c_0 and c_1 are the volume fractions of the matrix and the inclusions, respectively, and $\langle \cdot \rangle$ denotes a volume average over a given domain. Let us assume that the average deformation state of all inclusions is simulated by a single inclusion of domain ω_1^* embedded in a fictitious matrix occupying a domain ω_0^*. Hence, one needs to solve an equivalent inclusion problem (EIP) over a domain $\omega^* = \omega_0^* \cup \omega_1^*$ in which the volume fraction of the inclusion is infinitesimal: $\frac{V(\omega_1^*)}{V(\omega^*)} \ll 1$. It is further assumed that the surrounding, fictitious matrix is given the properties of the actual matrix. The displacement field $\boldsymbol{u}(\boldsymbol{x})$ through ω^* is the solution of the following boundary value problem:

$$\begin{cases} \operatorname{div}(\boldsymbol{\sigma}) = 0, \quad \forall \boldsymbol{x} \in \omega^* & \text{(equilibrium)} \\ \boldsymbol{u}(\boldsymbol{x}) = \boldsymbol{\varepsilon}^{\infty} \cdot \boldsymbol{x} \quad \forall \boldsymbol{x} \in \partial\omega^* & \text{(displacement B.C.)} \\ \boldsymbol{\varepsilon}(\boldsymbol{x}) = \frac{1}{2}(\nabla \boldsymbol{u}(\boldsymbol{x}) + \nabla^T \boldsymbol{u}(\boldsymbol{x})) & \text{(kinematics)} \\ \text{(constitutive equations)} \end{cases} \tag{6}$$

where $\operatorname{div}(\boldsymbol{\sigma})$ is the divergence of the stress tensor and $\boldsymbol{\varepsilon}^{\infty}$ is the imposed far-field strain, defined so as to account for interactions between inclusions. In the proposed model, the system of Eq. (6) is solved "exactly" by the FE method, see Section 2. This allows us to deal with the nonlinear constitutive behavior of the individual phases. In the model, the average strain of the inclusions of the real composite is assumed equal to the average strain over the single inclusion in the EIP: $\langle \boldsymbol{\varepsilon} \rangle_{\omega_1} = \langle \boldsymbol{\varepsilon} \rangle_{\omega_1^*}$.

A very simple homogenization scheme is obtained by taking the macroscopic strain as far-field strain: $\boldsymbol{\varepsilon}^{\infty} = \bar{\boldsymbol{\varepsilon}}$. This corresponds to an extended dilute model, denoted by Dilute/FE1. This model is suitable for very low volume fractions of inclusions, as interactions between inclusions are not accounted for. The matrix average strain is then computed according to Eq. (5). However, this paper deals with composites with a higher volume fraction of reinforcement (up to 35%). Therefore, an extended Mori-Tanaka scheme (MT/FE1) is considered, in which the average strain in the actual matrix is used as far-field strain on the EIP, according to Benveniste's interpretation of the Mori-Tanaka scheme (Benveniste, 1987): $\boldsymbol{\varepsilon}^{\infty} = \langle \boldsymbol{\varepsilon} \rangle_{\omega_0}$. As the matrix average strain is a priori unknown, iterations over the values of $\langle \boldsymbol{\varepsilon} \rangle_{\omega_0}$ are needed, each of them requiring the FE resolution of the EIP and leading to an updated value of $\langle \boldsymbol{\varepsilon} \rangle_{\omega_1}$, until Eq. (5) is satisfied. Therefore, the M-T scheme is much more computer time demanding than the dilute model. The M-T scheme coupled with the FE solution of the EIP is schematically depicted in Fig. 2.

Once the strain partitioning is determined, the average stress in each phase of the original RVE must be computed. Similarly to the average strain, the inclusion average stress is easily extracted from the FE computation: $\langle \boldsymbol{\sigma} \rangle_{\omega_1} = \langle \boldsymbol{\sigma} \rangle_{\omega_1^*}$. However, the matrix average stress $\langle \boldsymbol{\sigma} \rangle_{\omega_0}$ cannot be directly extracted from the FE computation, as the matrix phase of the EIP is a fictitious one, which should not be confused with the matrix phase in the real composite although both matrices have the same constitutive behavior and properties. At this point, a modeling assumption must be introduced, which consists in the definition of a homogeneous comparison material for the matrix phase in the real composite. In the present model, the constitutive box of the matrix material is simply called with the current average strain, average strain increment and state variables of the real matrix. The stress that the box computes is taken

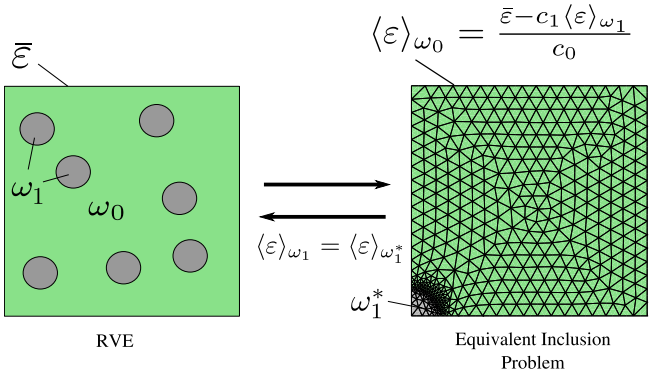

Fig. 2. The Mori-Tanaka scheme coupled with a FE solution of the equivalent inclusion problem (EIP). The inclusion average strain $\langle \boldsymbol{\varepsilon} \rangle_{\omega_1}$ is given by the volume average of the strain in the inclusion of the EIP subjected to the matrix average strain $\langle \boldsymbol{\varepsilon} \rangle_{\omega_0}$ as far-field strain. The latter is computed iteratively so that $\bar{\boldsymbol{\varepsilon}} = c_0 \langle \boldsymbol{\varepsilon} \rangle_{\omega_0} + c_1 \langle \boldsymbol{\varepsilon} \rangle_{\omega_1}$.

as an estimate of the average stress of the matrix. This strategy was also adopted by Doghri and Ouaar (2003) in the incremental tangent M-T scheme, in which case good predictions of the effective response of the composite were obtained. Finally, the macroscopic stress is defined as the stress average over the composite:

$$\bar{\boldsymbol{\sigma}} \equiv c_0 \langle \boldsymbol{\sigma} \rangle_{\omega_0} + c_1 \langle \boldsymbol{\sigma} \rangle_{\omega_1}. \tag{7}$$

3.2. Numerical procedure

Consider a time interval $[t_n, t_{n+1}]$. The macroscopic strain $\bar{\boldsymbol{\varepsilon}}$ is known, as well as all history variables at t_n. We aim to compute the macroscopic stress $\bar{\boldsymbol{\sigma}}_{n+1}$. The homogenization procedure according to the M-T model reads as follows (the subscript $n+1$ is omitted for simplicity):

- Initialization: $\langle \boldsymbol{\varepsilon} \rangle_{\omega_0} \leftarrow \bar{\boldsymbol{\varepsilon}}$.
- Iteration (r) (upper index (r) omitted for simplicity):
  1. Apply displacement boundary conditions to the EIP following (6)b.
  2. Solve the EIP by the FE method for the considered time increment, starting from the deformed state at t_n.
  3. Compute the average strain in the inclusions of the actual composite as

$$\langle \boldsymbol{\varepsilon} \rangle_{\omega_1} = \langle \boldsymbol{\varepsilon} \rangle_{\omega_1^*} = \frac{1}{V(\omega_1^*)} \sum_{k=1}^{N_k} \boldsymbol{\varepsilon}_k V_k, \tag{8}$$

     where $\boldsymbol{\varepsilon}_k$ is the strain at the integration point k, V_k is the volume associated with the integration point k, and N_k the total number of integration points in the discretized domain ω_1^*. The inclusion average stress is computed in a similar way.
  4. Check compatibility of average strain in the inclusions by computing residual:

$$\boldsymbol{R} = \frac{\bar{\boldsymbol{\varepsilon}} - c_1 \langle \boldsymbol{\varepsilon} \rangle_{\omega_1}}{c_0} - \langle \boldsymbol{\varepsilon} \rangle_{\omega_0}. \tag{9}$$

  5. If $|\boldsymbol{R}| < \mathrm{TOL}$ then exit the loop.
  6. Else: new iteration with new $\langle \boldsymbol{\varepsilon} \rangle_{\omega_0}$:

$$\langle \boldsymbol{\varepsilon} \rangle_{\omega_0} \leftarrow \langle \boldsymbol{\varepsilon} \rangle_{\omega_0} + \boldsymbol{R}. \tag{10}$$

- After convergence, the average matrix stress $\langle \boldsymbol{\sigma} \rangle_{\omega_0}$ is approximated by calling the constitutive box with the average strain $\langle \boldsymbol{\varepsilon} \rangle_{\omega_0}$, average strain increment $\langle \Delta \boldsymbol{\varepsilon} \rangle_{\omega_0}$ and the history variables at t_n. Finally, the macroscopic stress $\bar{\boldsymbol{\sigma}}$ is computed as the average stress over the composite (Eq. (7)).

For the Dilute/FE1 model, iterations on the far-field strain are not required and a unique FE computation on the single inclusion cell is sufficient to compute the particle average strain and stress according to relation (8). Next, the matrix average strain is computed with Eq. (5). The computations of the matrix average stress and the macroscopic stress are identical to the M-T model.

At this point, several aspects of the proposed approach should be emphasized:

- The procedure is fully history-dependent: the deformation state at each integration point in the FE discretization as well as the current matrix average state depend on the corresponding state at the previous time step. Consequently, any loading condition, even non-monotonic or non-proportional may be considered.
- One should distinguish two relatively independent tasks of the model. The first task is to estimate the inclusion and matrix average strains according to an extended Mori-Tanaka (or dilute) model, for a given macroscopic strain tensor $\bar{\boldsymbol{\varepsilon}}$. Next, it is still required to determine the average stress in each phase. The inclusion average stress may be directly extracted from the FE simulation. On the other hand, computing the average stress for the nonlinear matrix is not trivial, as the model provides only the matrix average strain. Unfortunately, valid estimates of higher order moments of the strain field are, to the authors' knowledge, not yet available in the framework of incremental MF models. Therefore, a simple, first order approach is adopted following Doghri and Ouaar (2003). As shown in the next section, the first order approximation is successful when the strain partitioning is properly predicted.
- The computation of the average stress in each phase affects only the effective response of the composite, not the prediction of the strain partitioning. This holds provided that all components of the macroscopic strain are given. However, when simulating a uniaxial tension test for example, outer iterations are required in order to compute the macro transverse strains. In this case, the two modeling parts described above are coupled, and it might become difficult to assess the M-T assumption alone. In this work, this problem is circumvented by considering strain driven loading conditions only. Uniaxial and plane strain loading conditions are reproduced by imposing at each time step in the MF model the macro strain tensor from a given multiparticle simulation with same material and topological parameters.

4. Results

The dilute and M-T models coupled with the FE solution of the EIP are used to simulate two-phase composites consisting of an elasto-plastic matrix reinforced by linear elastic inclusions. The predictions of the mean-field models are compared to reference results from FE computations on representative cells containing a random arrangement of multiple inclusions. Uniaxial and plane strain loading are successively applied to the multiparticle cells. The average of the macroscopic strain over a RVE computed at each time step provides the loading history for the corresponding MF models. Therefore, both reference and MF results correspond to the same macroscopic strain history, consistently with a strain driven homogenization procedure.

4.1. Two-phase steel under tension/compression tests

Consider a two-phase steel made of a ferritic matrix reinforced by martensitic inclusions. The ellipsoidal inclusions are characterized by Young's modulus and Poisson's ratio $E_1 = 200$ GPa and $\nu_1 = 0.3$. The matrix elastic constants are $E_0 = 220$ GPa and $\nu_0 = 0.3$. The elasto-plastic behavior of the matrix is described by classical J_2 theory with power law representation of hardening:

$$\sigma_y = \sigma_{y0} + k p^m, \tag{11}$$

where σ_{y0} and σ_y are the initial and current yield stresses, respectively, k and m are hardening parameters and p is the accumulated plastic strain. Here, the initial yield stress is $\sigma_{y0} = 300$ MPa and the hardening parameters are $k = 1130$ MPa and $m = 0.31$. The ellipsoids long diameter are aligned with the direction of traction. The macroscopic strain (dilute model) and the average matrix strain (M-T model) are successively applied to the boundaries of the single inclusion cell. The equivalent stress σ_{eq} in the single inclusion for both models is compared to the reference result in Fig. 3. It is observed that the single inclusion models underestimate the inclusion

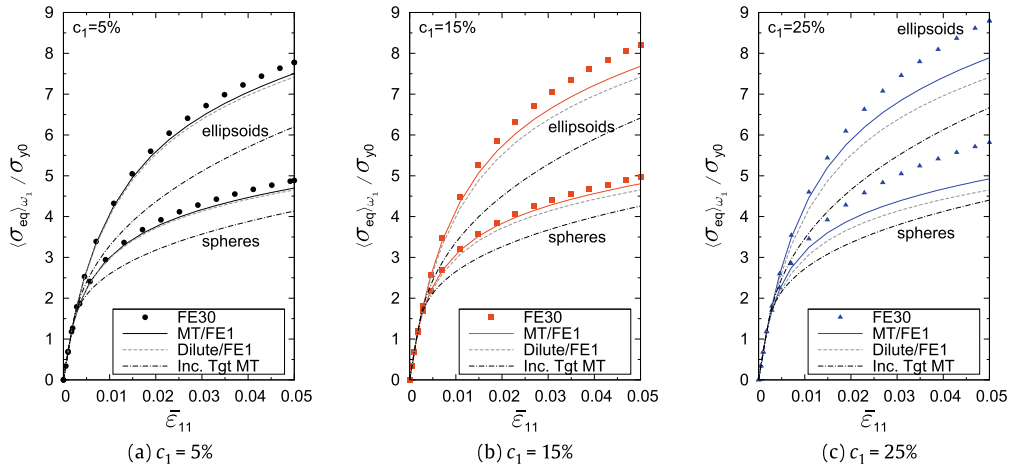

Fig. 3. Average equivalent stress in the inclusions of a two-phase steel for different volume fractions of the reinforcing phase. The multiparticle, FE predictions (FE30) correspond to a uniaxial tension test, while the predictions of the coupled Mori-Tanaka/FE model (MT/FE1) and coupled dilute/FE model (Dilute/FE1) were obtained imposing the same strain history as in the multiparticle simulation. For comparison, the predictions of the incremental tangent model of Pierard and Doghri (2006b) (Inc. Tgt MT) are also shown for uniaxial tension.

stress whatever the inclusion volume fraction and shape, the discrepancy increasing with the volume fraction. In the case of spherical inclusions, the discrepancy between the MT/FE1 and multiparticle models is smaller than 5% for $c_1 = 5\%$ and $c_1 = 15\%$, but it rises up to 15% with 25% volume fraction of inclusion. The predictions are a little less accurate in the case of ellipsoidal inclusions. On the other hand, the dilute (Dilute/FE1) assumption gives softer responses than the M-T assumption, as expected, and is therefore not suited for volume fractions larger than 5%. For comparison, results obtained with an incremental M-T scheme (as presented in Pierard and Doghri (2006b)) are also shown. In this case, the EIP is solved semi-analytically, see Eq. (16) and Appendix B.1. As mentioned in the introduction, the predictions of this scheme underestimate the inclusion stress for all considered volume fractions and shapes, and are even softer than the predictions of the Dilute/FE1 model.

The macroscopic stress of the composite based on the single inclusion modeling is computed according to Eq. (7), which implies the definition of a comparison material for the matrix. It is clear from Fig. 4(a) that the proposed M-T model (MT/FE1) correctly predicts the overall response of the composite up to 25% of spherical inclusions during the whole cycle of deformation. Actually, macroscopic predictions are more accurate than the predictions of the inclusion stress, even with $c_1 = 25\%$ for which the inaccuracy of the MT/FE1 model was rather important (Fig. 3(c)). The underestimation of the inclusions strain is compensated by a slight overestimation of the matrix strain, which combined with the present choice of reference material provides accurate prediction of the macroscopic stress. This is no longer the case at 35%, where the effective response is clearly overestimated by the M-T model. In the case of ellipsoidal inclusions aligned with the direction of traction (Fig. 4(b)), agreement between the macroscopic responses is observed for all volume fractions up to 25%. In any case, the M-T approach overestimates the effective response, and the accuracy decreases with the volume fraction of inclusions. Here, the predictions of the incremental M-T model of Pierard and Doghri (2006b) are not shown for the sake of clarity.

A similar study is conducted when applying plane strain tension/compression on the same multiparticle cells, with $\bar{\boldsymbol{\varepsilon}}$ of the form:

$$\bar{\boldsymbol{\varepsilon}} = \begin{pmatrix} \bar{\varepsilon}_{11} & 0 & 0 \\ 0 & \bar{\varepsilon}_{22} & 0 \\ 0 & 0 & 0 \end{pmatrix} \tag{12}$$

and such that $\bar{\sigma}_{22} = 0$. Fig. 5 shows the inclusion response for different inclusion volume fractions and shapes. Again, the dilute model

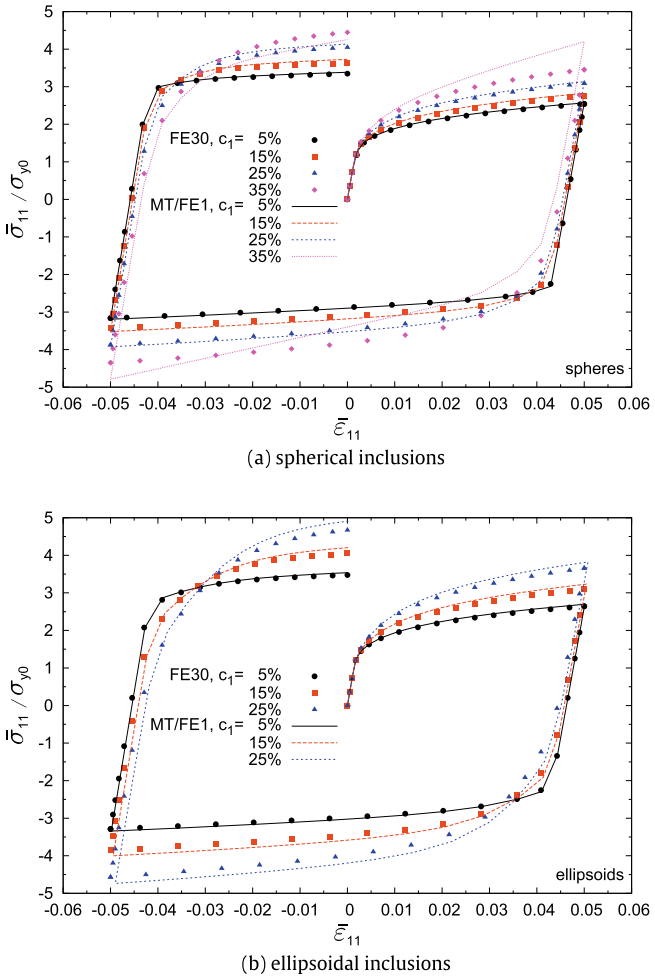

Fig. 4. Effective response of a two-phase steel reinforced by spherical (a) or aligned, ellipsoidal (b) inclusions, for different volume fractions of the reinforcing phase. The multiparticle, FE predictions (FE30) correspond to a uniaxial tension test, while the predictions of the coupled Mori-Tanaka/FE model (MT/FE1) and coupled dilute/FE model (Dilute/FE1) were obtained imposing the same strain history as in the multiparticle simulation.

gives softer predictions than the M-T model, the latter being satisfying for spherical inclusions up to $c_1 = 15\%$. Predictions are less accurate for ellipsoidal inclusions. Similarly to the uniaxial tension test, the incremental M-T scheme based on an approximate solution of the EIP yields the softest (and least accurate) predictions, especially for ellipsoidal inclusions. On the other hand, the macroscopic response given by the coupled M-T/FE model performs well whatever the volume fraction and shape (Fig. 6). On the contrary of the uniaxial case, the prediction is still very accurate at 35% volume fraction of inclusions.

4.2. Metal matrix composite under uniaxial tension

The single inclusion modeling is now applied to a metal matrix composite (MMC) under uniaxial tension. The inclusions are ellipsoidal with an aspect ratio $\alpha = 3$ and have a linear elastic behavior with elastic constants $E_1 = 400$ GPa and $\nu_1 = 0.2$. The matrix is characterized by Young's modulus and Poisson's ratio $E_0 = 70$ GPa and $\nu_0 = 0.33$, and the equivalent stress is related to the accumulated plastic strain according to the power law:

$$\sigma_{eq} = kp^m, \tag{13}$$

with $k = 400$ MPa. Two hardening exponents are successively considered: $m = 0.05$ and $m = 0.4$. The volume fraction of inclusions is 25%, which was a threshold volume fraction for the validity of the single inclusion model in Section 4.1. This composite was previously studied by Pierard et al. (2007) using direct FE simulations on RVE's with 30 inclusions and periodic boundary conditions, and all reference results are extracted from that paper. The macroscopic response of the MMC characterized by $m = 0.05$ is plotted in Fig. 7(a),(b) for two different configurations: in Fig. 7(a) the fibers are aligned with the direction of traction, while the loading is applied transversely to the fibers in Fig. 7(b). The M-T and dilute models give very similar (and accurate) predictions of the effective stress in both configurations. In the longitudinal case, the dilute model gives better predictions than the M-T model. For a higher matrix hardening exponent (Fig. 7(c) and (d)), the discrepancy between the reference and approximate models increases, so does the difference between the dilute and Mori-Tanaka model. The latter is closer to the reference solution, and the maximal relative error in the transverse case is about 7%. However, it has been shown previously that a good macroscopic prediction may be obtained despite a poor prediction of the local strains. This is also the case of this

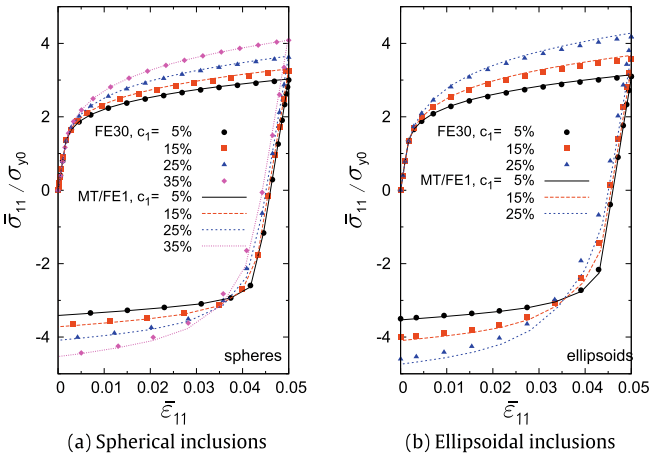

(a) Spherical inclusions (b) Ellipsoidal inclusions

Fig. 6. Effective response of a two-phase steel reinforced by spherical (a) or aligned, ellipsoidal (b) inclusions, for different volume fractions of the reinforcing phase. The multiparticle, FE predictions (FE30) correspond to plane strain tension/compression ($\bar{\varepsilon}_{33} = 0$), while the predictions of the coupled Mori-Tanaka/FE model (MT/FE1) and coupled dilute/FE model (Dilute/FE1) were obtained imposing the same strain history as in the multiparticle simulation.

MMC: Fig. 8(a) shows that the equivalent stress computed on the single inclusion is far from the reference inclusion response. The accumulated plastic strain is plotted in Fig. 8(b) for the different models. In the case of the MF approaches, this quantity is computed from the comparison material, *not* from a volumetric average over the matrix of the single inclusion problem. Again, an important discrepancy between the reference and MF results is observed. Note the very similar predictions of the accumulated plastic strain of the M-T and dilute models.

5. Semi-analytical approximate solutions of the equivalent inclusion problem

The previous section showed that a Mori-Tanaka assumption can reasonably be used for the modeling of two-phase elasto-plastic composites for low to moderate volume fraction of reinforcement, provided that the EIP is solved "exactly". Semi-analytical mean-field schemes based on the M-T assumption should also provide valid predictions if they can relate on an acceptable semi-ana-

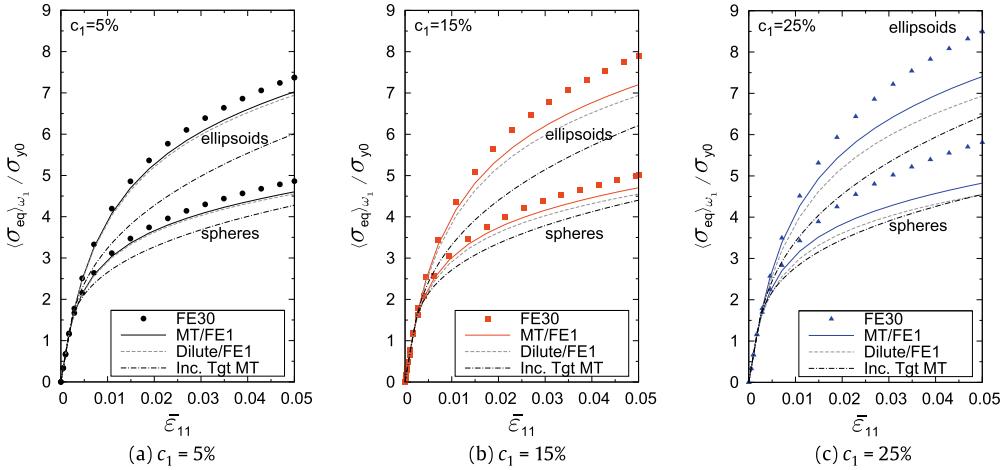

(a) c_1 = 5% (b) c_1 = 15% (c) c_1 = 25%

Fig. 5. Average equivalent stress in the inclusions of a two-phase steel for different volume fractions of the reinforcing phase. The multiparticle, FE predictions (FE30) correspond to a plane strain tension test, while the predictions of the coupled Mori-Tanaka/FE model (MT/FE1) and coupled dilute/FE model (Dilute/FE1) were obtained imposing the same strain history as in the multiparticle simulation. For comparison, the predictions of the incremental tangent model of Pierard and Doghri (2006b) (Inc. Tgt MT) are also shown for plane strain tension.

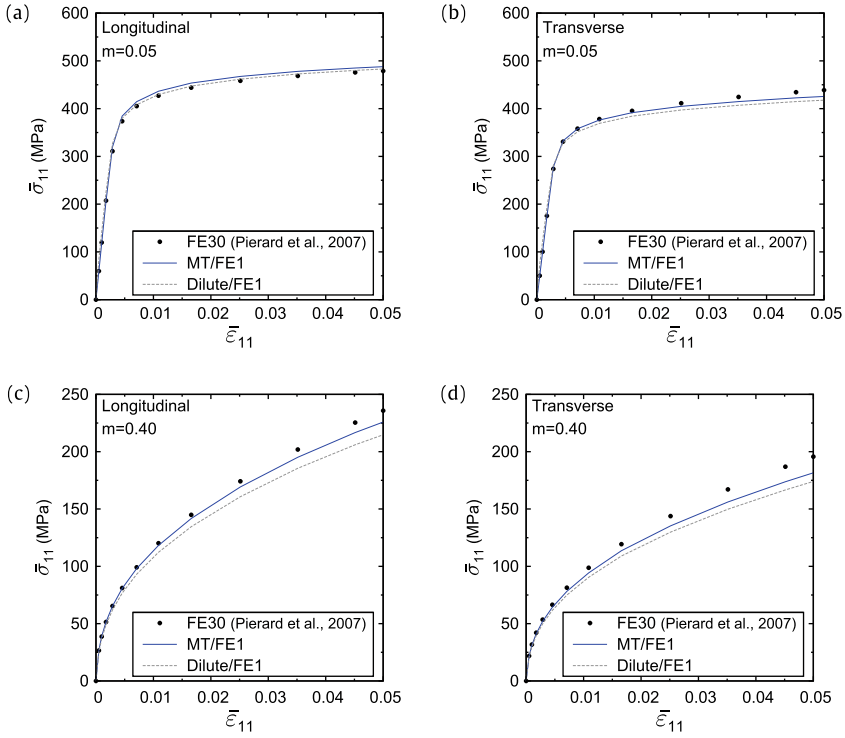

Fig. 7. Macroscopic response of a metal matrix composite for two hardening exponents: $m = 0.05$ ((a) and (b)) and $m = 0.40$ ((c) and (d)). Comparison between FE results on multiparticle cells under uniaxial tension of Pierard et al. (2007) (FE30) and estimates for the same macroscopic strain history obtained with the coupled Mori-Tanaka/FE model (MT/FE1) and the coupled dilute/FE model (Dilute/FE1). Fibers are either aligned with the direction of traction ((a) and (c)) or perpendicular to the direction of traction ((b) and (d)).

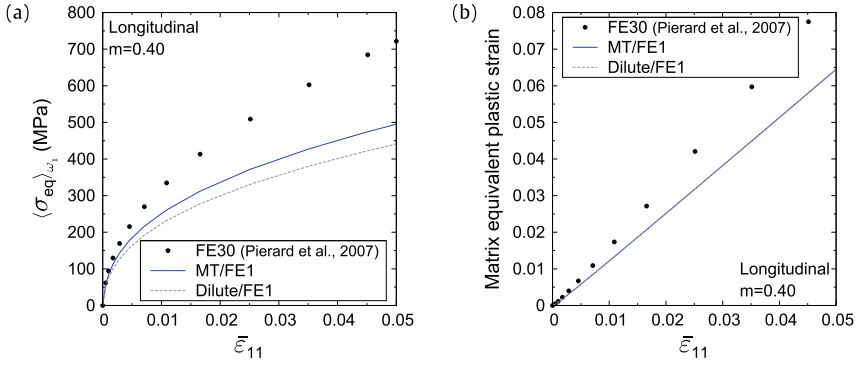

Fig. 8. Metal matrix composite with hardening exponent $m = 0.40$ and fibers aligned with the direction of traction. Comparison between FE results on multiparticle cells under uniaxial tension of Pierard et al. (2007) (FE30) and estimates for the same macroscopic strain history obtained with the coupled Mori-Tanaka/FE model (MT/FE1) and the coupled dilute/FE model (Dilute/FE1). (a) Average of the equivalent stress in the inclusion. (b) Average accumulated plastic strain in the matrix.

lytical localization equation relating the inclusion average strain to the far-field strain applied to the EIP. In an incremental approach, this problem can be reformulated as follows: Find the fourth-order strain concentration tensor $\boldsymbol{H}^{\epsilon}$ such that:

$$\langle\dot{\boldsymbol{\varepsilon}}\rangle_{\omega_1^*} = \boldsymbol{H}^{\epsilon} : \dot{\boldsymbol{\varepsilon}}^{\infty}. \tag{14}$$

When both phases are linear elastic, the strain concentration tensor is given by Eshelby's solution of the isolated inclusion problem:

$$\boldsymbol{H}^{\epsilon} = \left\{\boldsymbol{I} + (\boldsymbol{S}(\boldsymbol{C}_0^{\mathrm{el}}) : (\boldsymbol{C}_0^{\mathrm{el}})^{-1}) : (\boldsymbol{C}_1^{\mathrm{el}} - \boldsymbol{C}_0^{\mathrm{el}})\right\}^{-1}, \tag{15}$$

where $\boldsymbol{C}_0^{\mathrm{el}}$ and $\boldsymbol{C}_1^{\mathrm{el}}$ are Hooke's operators for the matrix and inclusion phases, respectively, and $\boldsymbol{S}$ is Eshelby's tensor, which only depends on the matrix stiffness and the inclusion shape. When one of the phases behaves nonlinearly, such exact expression for the strain concentration tensor is not available, and approximate methods must be used.

Following Hill (1965), incremental MF models assume that the strain (rate) concentration tensor is form similar to its linear elastic expression (15), taking homogeneous, reference *tangent* operators for the nonlinear phases:

$$\boldsymbol{H}^{\epsilon} = \{\boldsymbol{I} + (\boldsymbol{S}(\widehat{\boldsymbol{C}}_0) : \widehat{\boldsymbol{C}}_0^{-1}) : (\widehat{\boldsymbol{C}}_1 - \widehat{\boldsymbol{C}}_0)\}^{-1}. \tag{16}$$

For the elasto-plastic composite considered in this paper, $\widehat{\boldsymbol{C}}_0$ is a reference operator for the elasto-plastic matrix, and $\widehat{\boldsymbol{C}}_1$ is Hooke's operator of the inclusion. The problem of finding the "right" strain concentration tensor is thus reduced to the definition of a proper reference operator for the elasto-plastic matrix in the isolated inclusion problem. In the incremental M-T scheme proposed by Pierard and Doghri (2006b), the reference tangent operator is given by

the isotropic decomposition of the algorithmic tangent operator computed for the average strain of the matrix, see Appendix B.1. The corresponding strain concentration tensor will be further denoted by $H^{\mathrm{Iso,spe}}$. However, this scheme was shown to underestimate the inclusion stress when applied to the two-phase steel of the previous section (see also Delannay et al., 2007; Pierard et al., 2007). Therefore, Delannay et al. (2007) proposed a modified version of this scheme based on a heuristic approach. The authors proposed to modify the reference tangent operator of the incremental M-T scheme by incorporating a dependence on the ratio of equivalent stress in the inclusion and the matrix (Appendix B.2). In this way, accurate predictions of the macroscopic response *and* inclusion response were obtained when applied to the present two-phase steel. However, the method remains heuristic and is a priori not predictive for other composite materials. In the following, the strain concentration tensor obtained with this model will be denoted $H^{\mathrm{Iso,heur}}$. In both schemes, the tangent operators in Eq. (16) are isotropic. As a consequence, when the inclusions are spherical, Eshelby's tensor and the strain concentration tensor are isotropic.

Alternatively, the strain concentration tensor in Eq. (14) can be computed numerically by a perturbation method combined with the FE solution of the EIP. First, relation (14) is integrated over a given time increment $[t_n, t_{n+1}]$, which yields (subscript $(n+1)$ omitted for simplicity):

$$\langle \Delta\boldsymbol{\varepsilon}\rangle_{\omega_1^*} = \boldsymbol{H}^{\epsilon}_{n+\alpha} : \Delta\boldsymbol{\varepsilon}^{\infty}, \tag{17}$$

where a generalized mid-point rule is used:

$$(\bullet)_{n+\alpha} = (\bullet)_{(t=t_{n+\alpha})}, \quad t_{n+\alpha} = (1-\alpha)t_n + \alpha t_{n+1}, \quad \alpha \in [0,1]. \tag{18}$$

Seeing the inclusion strain increment as a nonlinear function of the far-field strain increment: $\langle \Delta\boldsymbol{\varepsilon}\rangle_{\omega_1^*} = f(\Delta\boldsymbol{\varepsilon}^{\infty})$, the following expression of the strain concentration tensor is found:

$$\boldsymbol{H}^{\epsilon}_{n+\alpha} = \left(\frac{\partial\langle \Delta\boldsymbol{\varepsilon}\rangle_{\omega_1^*}}{\partial\Delta\boldsymbol{\varepsilon}^{\infty}}\right)_{n+\alpha}. \tag{19}$$

The pertubation method consists in estimating the derivatives in Eq. (19) by finite differences, successively pertubating one of the 6 different components of the applied far-field strain increment at $t_{n+\alpha}$. Here, a mid-point integration rule is used: $\alpha = \frac{1}{2}$. A uniaxial tension test is performed on a unit cell along direction 1 up to $\varepsilon_{11}^{\infty} = 5\%$, with 100 time increments. The cell contains a single spherical or ellipsoidal inclusion of volume fraction 0.1% placed at its center. The FE discretization has been described in Section 2. It was checked that the relative error on the inclusion strain increment computed according to Eq. (17) is less than 3% at the end of the loading. The reference strain concentration tensor obtained with the pertubation method will be denoted $\boldsymbol{H}^{\mathrm{FE}}$.

In order to compare the numerical strain concentration tensor $\boldsymbol{H}^{\mathrm{FE}}$ with its counterparts provided by MF models, its isotropic and transversely isotropic projections are also computed. The isotropic projection of $\boldsymbol{H}^{\mathrm{FE}}$, noted $\boldsymbol{H}^{\mathrm{FE,Iso}}$, is computed according to the general method (see Appendix A.1). The method yields two scalars κ_t^H and μ_t^H, so that:

$$\boldsymbol{H}^{\mathrm{FE,Iso}} = 3\kappa_t^H \boldsymbol{I}^{\mathrm{vol}} + 2\mu_t^H \boldsymbol{I}^{\mathrm{dev}}. \tag{20}$$

Expressions of κ_t^H and μ_t^H are given by (A.4) and (A.5).

The transverse isotropic part $\boldsymbol{H}^{\mathrm{FE,TrIso}}$ of the strain concentration tensor is found by a general method proposed by Walpole (1981) and described in Appendix A.2. The transversely isotropic part is totally described by 6 coefficients H_i, so that

$$\begin{aligned}\boldsymbol{H}^{\mathrm{FE,TrIso}} &= \sum_{i=1,6} H_i \boldsymbol{E}_i = (\boldsymbol{E}_1 :: \boldsymbol{H}^{\mathrm{FE}})\boldsymbol{E}_1 + (\boldsymbol{E}_2 :: \boldsymbol{H}^{\mathrm{E}})\boldsymbol{E}_2 \\ &+ \frac{1}{2}(\boldsymbol{E}_3 :: \boldsymbol{H}^{\mathrm{FE}})\boldsymbol{E}_3 + \frac{1}{2}(\boldsymbol{E}_4 :: \boldsymbol{H}^{\mathrm{FE}})\boldsymbol{E}_4 + \frac{1}{2}(\boldsymbol{E}_6 :: \boldsymbol{H}^{\mathrm{FE}})\boldsymbol{E}_5 \\ &+ \frac{1}{2}(\boldsymbol{E}_5 :: \boldsymbol{H}^{\mathrm{FE}})\boldsymbol{E}_6 \end{aligned} \tag{21}$$

where the six fourth-order tensors $\boldsymbol{E}_i$ are given by Eqs. (A.12)–(A.17). The direction of anisotropy $\boldsymbol{w}$ is supposed to be aligned with the direction of the uniaxial tension: $\boldsymbol{w} = \boldsymbol{e}_1$.

5.1. Prediction of the inclusion stress

The approximated strain concentration tensors $\boldsymbol{H}^{\mathrm{Iso,spe}}$ and $\boldsymbol{H}^{\mathrm{Iso,heur}}$ are now compared to the reference one $\boldsymbol{H}^{\mathrm{FE}}$ and to its isotropic and transverse isotropic projections. To this end, the inclusion response of an isolated inclusion system in uniaxial tension is computed based on the different strain concentration tensors in Fig. 9. The material properties are those of the two-phase steel of Section 4.1, and the inclusion is spherical, with a volume fraction equal to 0.1%. No homogenization is performed here, only the localization problem in the EIP under uniaxial traction is considered. The strain concentration tensors relate the far-field strain increment to the average inclusion strain increment, and the average stress in the inclusion is computed according to Hooke's law. Direct FE computation on the single inclusion cell provides the reference prediction of the average inclusion stress, denoted by (FE) in the figure. It was checked that the same stress–strain curve is found when using the numerical strain concentration tensor $\boldsymbol{H}^{\mathrm{FE}}$ to compute the inclusion strain increment. It is obvious from the figure that the isotropic projection of the reference strain concentration tensor $\boldsymbol{H}^{\mathrm{FE,Iso}}$ gives far too stiff predictions of the inclusion stress. Hence the "true" strain concentration tensor is *not* isotropic. On the other hand, its transverse isotropic projection $\boldsymbol{H}^{\mathrm{FE,TrIso}}$ gives predictions almost identical to the reference curve, so that the latter can be seen as transversely isotropic, which is most probably correlated to the present loading. The strain concentration tensor given by the incremental scheme of Pierard and Doghri (2006b), $\boldsymbol{H}^{\mathrm{Iso,spe}}$ underestimates the inclusion response $\langle\sigma_{11}\rangle_{\omega_1^*}$. Therefore, the inaccuracy of this model in predicting the inclusion stress during a homogenization procedure is clearly related to the inaccurate solution of the EIP associated with this scheme, as the M-T assumption alone gives acceptable prediction of the inclusion response at low volume fraction, see Fig. 3(a) and (b). Note however that the slope of the curve far from the elastic–plastic transition is correctly predicted. Finally, the strain concentration tensor of the incremental MF model is modified according to the heuristic approach of Delannay et al. (2007), taking $c_1 = 0.1\%$ in Eq. (B.5). Other parameters in Eq. (B.5) are given the same value as in Delannay et al. (2007): $A_0 = 7.5$ and $V_{max} = 0.53$. It is found that this strain concentration tensor $\boldsymbol{H}^{\mathrm{Iso,heur}}$ gives the best prediction of the inclusion stress $\langle\sigma_{11}\rangle_{\omega_1^*}$, in spite of the use of an isotropic tensor.

An important observation is that there exists at least *two* different strain concentration tensors, one of them being isotropic, which yield an accurate prediction of the inclusion response in the single inclusion problem: the reference, FE one, and the strain concentration tensor of the heuristically modified M-T scheme of Delannay et al. (2007). However, the latter does *not* correspond to the isotropic projection of the FE strain concentration tensor (by means of the general isotropisation method).

A similar study is conducted in the case of the MMC of Section 4.2, with strain hardening exponent $m = 0.4$. The isolated inclusion is ellipsoidal with aspect ratio $\alpha = 3$, and aligned with the direction of traction. Comparison of the average inclusion stress in the longitudinal and transverse directions as predicted using several strain

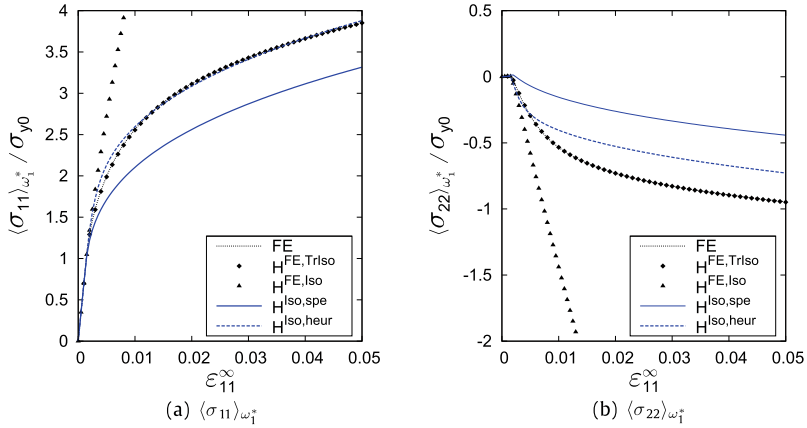

Fig. 9. Average inclusion stress in the Equivalent Inclusion Problem (EIP) as predicted using different strain concentration tensors for a two-phase steel under uniaxial tension along direction 1. The single inclusion is spherical. Predictions of the inclusion average stress are compared to the reference result provided by direct FE resolution of the single inclusion problem.

concentration tensors is presented in Fig. 10. Again, the numerical strain concentration tensor $\boldsymbol{H}^{\mathrm{FE}}$ is found to be almost transversely isotropic. Note that the slight difference with the reference curve is due to some inaccuracy in the computation of the numerical strain concentration tensor at the very beginning of the loading, and not to the transverse isotropic projection. On the other hand, the isotropic projection of $\boldsymbol{H}^{\mathrm{FE}}$ gives far too stiff predictions. The strain concentration of the incremental MF scheme $\boldsymbol{H}^{\mathrm{Iso,spe}}$ underestimates the inclusion stress in Fig. 10(a), and stiffer predictions are obtained with its heuristic variant $\boldsymbol{H}^{\mathrm{Iso,heur}}$. Note however that we use the same fitting parameters as in the case of the two-phase steel. Better predictions are expected by choosing the fitting parameters carefully, but this is not the purpose of the present study.

5.2. Comparison of components of the strain concentration tensors

The study is pursued by comparing the coefficients of the isotropic or transversely isotropic strain concentration tensors individually. The numerical strain concentration tensor $\boldsymbol{H}^{\mathrm{FE}}$ is represented by its transversely isotropic projection, $\boldsymbol{H}^{\mathrm{FE,TrIso}}$, which is very close the original tensor, as shown previously. The different strain concentration tensors are represented by their symbolic form proposed by Walpole (1981) for transversely isotropic tensors (Appendix A.2):

$$\boldsymbol{H}^{\mathrm{TrIso}} = (H_1, H_2, H_3, H_4, H_5, H_6). \tag{22}$$

Isotropic tensors characterized by a volumetric term κ_t^H and a deviatoric term μ_t^H may be expressed under the same symbolic form:

$$\boldsymbol{H}^{\mathrm{Iso}} = \left(2\kappa_t^H + \frac{2}{3}\mu_t^H, \kappa_t^H + \frac{4}{3}\mu_t^H, 2\mu_t^H, 2\mu_t^H, \kappa_t^H - \frac{2}{3}\mu_t^H, \kappa_t^H - \frac{2}{3}\mu_t^H\right). \tag{23}$$

This (redundant) form is useful for the comparison of the isotropic and transversely isotropic projections.

The comparison of the 6 coefficients H_i is presented for 3 strain concentration tensors in Fig. 11 in the case of the two-phase steel. The transversely isotropic projection of $\boldsymbol{H}^{\mathrm{FE}}$ and the tensors obtained by mean-field approaches: the incremental M-T scheme ($\boldsymbol{H}^{\mathrm{Iso,spe}}$) and the modified version ($\boldsymbol{H}^{\mathrm{Iso,heur}}$). The largest difference is observed for the coefficients H_3 and H_4, which are directly related to the deviatoric term μ_t^H in isotropic tensors. However, the influence of these coefficients is difficult to assess in this case as the present far-field strain has no shear components. In general, the different tensors differ during the elasto-plastic transition, where the components of the heuristically modified tensor $\boldsymbol{H}^{\mathrm{Iso,heur}}$ are closer to those of the numerical tensor than the ones of $\boldsymbol{H}^{\mathrm{Iso,spe}}$: increasing the inclusion stress increment at this stage is precisely the purpose of the heuristic correction. Also note that H_5 differs from H_6 in the case of the transversely isotropic

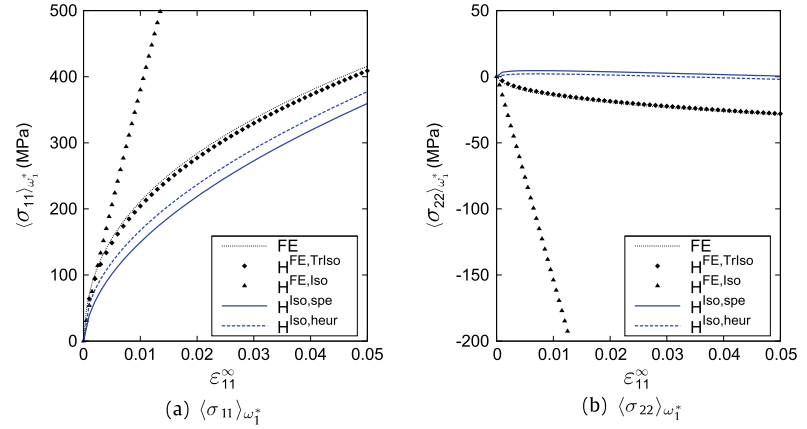

Fig. 10. Average inclusion stress in the Equivalent Inclusion Problem (EIP) as predicted using several strain concentration tensors for a metal matrix composite under uniaxial tension along direction 1. The single inclusion is ellipsoidal with aspect ratio $\alpha = 3$ and aligned with the direction of traction. Predictions of the inclusion average stress are compared to the reference result provided by direct FE resolution of the single inclusion problem.

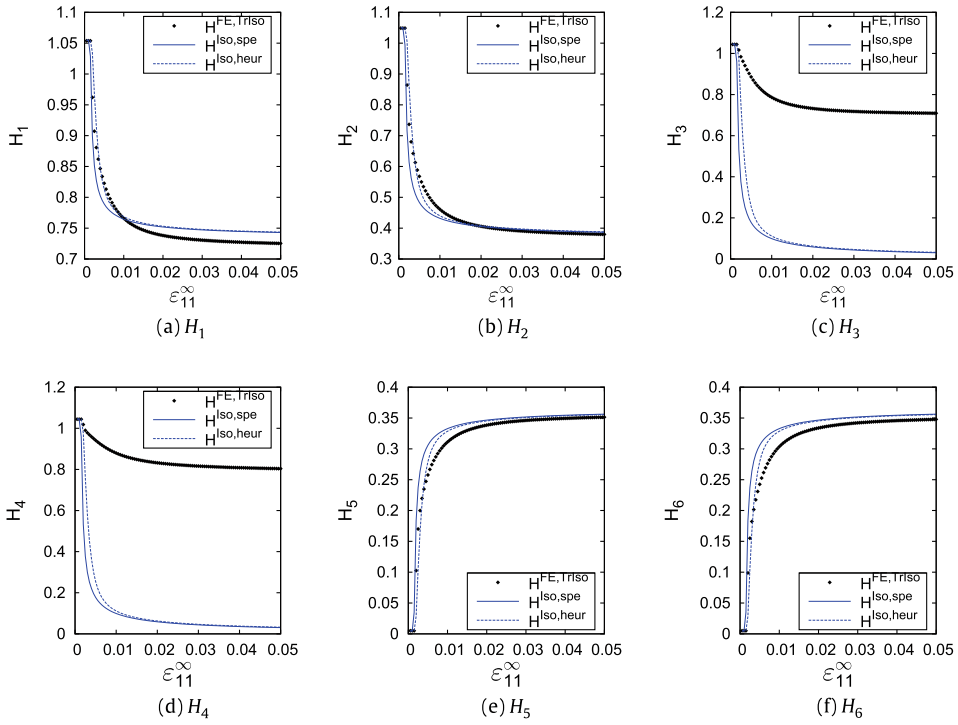

Fig. 11. Comparison of the 6 coefficients of the transversely isotropic projection of the strain concentration tensors computed by the perturbation method and two mean-field models: the incremental Mori-Tanaka scheme, and a heuristic variant, as a function of the far-field strain. The material parameters correspond to a two-phase steel.

projection of $\boldsymbol{H}^{\mathrm{FE}}$: this means that this numerical tensor is not exactly pair-symmetric.

6. Discussion and conclusions

A new procedure for evaluating the relevance of the single inclusion concept in the mean-field (MF) modeling of elasto-plastic composites was presented. The inclusions response is predicted based on the solution of a single inclusion isolated in an infinite medium having the properties of the matrix. This equivalent inclusion problem (EIP) is solved by the FE method, allowing field heterogeneities to take place in the fictitious matrix. In the extended Mori-Tanaka model (MT/FE1), the average of the strain in the actual matrix of the composite is taken as far-field strain. For comparison, a dilute assumption is also tested. Both mean-field models are fully coupled with a nonlinear FE analysis of the EIP. In addition to the scheme governing the strain partitioning among the phases (M-T or dilute), the effective predictions are also affected by the chosen comparison material for the nonlinear matrix which enables computing the average matrix stress from the average matrix strain. In general, these two assumptions are coupled (for instance in uniaxial tension). Here, such coupling is avoided by considering strain driven loading paths in the MF approach. The new method is applied to two different composites made of an elasto-plastic matrix reinforced by spherical or ellipsoidal elastic inclusions. Macroscopic deformation histories corresponding to non-monotonic uniaxial and plane strain tension/compression are successively considered. In all case, predictions of the MF approaches are compared to reference results obtained by FE simulations on cells containing about thirty inclusions.

It was found that the M-T assumption is able to simulate the effective response of such composites up to about 25% of inclusion volume fraction, provided that the single inclusion problem is solved "exactly". However, the predicted inclusion response is, in general, less accurate than the macroscopic one: the stress level in the single inclusion is underestimated by the mean-field model, the discrepancy increasing with the volume fraction of inclusions. This effect is, to a certain extent, compensated by the matrix prediction which raises the stress level in the effective response. This is due to a slight overestimation of the matrix average strain combined with the present comparison material for the matrix. It is also shown that a M-T hypothesis gives better prediction of the inclusion response than a dilute model. This was expected, as the dilute model is designed for very low volume fractions and does not take particle interactions into account. On the other hand, the M-T assumption accounts for particle interactions through the use of the average strain in the actual matrix as far-field strain. This particular choice is found to be relevant when applied to nonlinear composites. For higher volume fractions (from 25%) the single inclusion modeling yields very poor predictions of the inclusion response. This can be explained by plastic localization taking place between inclusions in the real composites, which is overlooked by the MF model.

The proposed MT/FE1 model cannot be used in practice as a constitutive law in larger scale simulation, as its computational time is much larger than that of any semi-analytical model, due to several FE computations required at each time step. Nevertheless, the study underlined the importance of an accurate solution of the equivalent inclusion problem for nonlinear materials. Therefore, the resolution of the EIP in the context of incremental MF schemes is studied. In incremental MF models, a semi-analytical strain concentration tensor for the EIP is constructed based on Eshelby's result written in rate form and using reference tangent operators for each phase. It is shown that solving the EIP with the strain concentration tensor of the incremental M-T scheme proposed by Pierard and Doghri (2006b) underestimates the inclusion strain. Therefore, the underestimation of the inclusion response in a composite homogenized with this model, as observed in Figs. 3 and 5 and already reported by Delannay et al. (2007), may be related to the use of an inaccurate solution of the localization problem in the EIP. This, in turn, is linked to the choice of the

comparison material for the elastic–plastic matrix. On the other hand, using the comparison material defined heuristically in Delannay et al. (2007) gives a very good prediction of the inclusion stress, both in the EIP (Fig. 9) and in the context of a M-T scheme (Delannay et al., 2007). Note that the reference operators defined in these two MF models are isotropic, leading to isotropic strain concentration tensors when the inclusions are spherical. However, it is shown that the numerical strain concentration tensor obtained by a pertubation method is close to transverse isotropy for a uniaxial loading, even for spherical inclusions. Unfortunately, this observation does not support the isotropisation of tangent operators commonly used in incremental MF schemes.

This study showed that one could take advantage of an accurate solution of the equivalent inclusion problem for nonlinear composite materials. This point is most of the time overlooked by recent models which rely on this solution in the linear elastic case, through the use of linear comparison composite. Here, we emphasize on its direct resolution in the nonlinear case. The final goal (not achieved yet) is to gain insight from the FE solution of the EIP – Figs. 9–11 – in order to enhance the predictive capabilities (no fitting parameters) of advanced nonlinear semi-analytical MF models. Next to the isolated inclusion modeling of the particles, modeling assumptions concern the definition of the applied far-field strain and the way of computing the matrix average stress from the average strain: both can be adapted to compensate the inaccuracy of the single inclusion modeling, in particular for high volume fractions of reinforcements. For instance, one could incorporate higher order moments of strain in the computation of the matrix average stress. A more detailed study of the influence of these two factors is left for future work.

Acknowledgements

L. Brassart and L. Delannay are mandated by the National Fund for Scientific Research (FNRS, Belgium). The authors gratefully acknowledge O. Pierard for providing the tools for microstructure generation. Computing facilities were made available through contract FRFC-2.4502.05 with FNRS.

Appendix A. Projection of fourth-order tensors

A.1. Extraction of isotropic part of anistropic tensors

Any isotropic fourth-order tensor can always be written as the sum of two other tensors representing its volumetric and deviatoric parts:

$$\boldsymbol{C}^{\mathrm{Iso}} = 3\kappa \boldsymbol{I}^{\mathrm{vol}} + 2\mu \boldsymbol{I}^{\mathrm{dev}}, \tag{A.1}$$

where κ and μ are arbitrary scalars. When $\boldsymbol{C}^{\mathrm{Iso}}$ is a stiffness tensor, these scalars are the bulk and shear moduli, respectively. The isotropic part of an anisotropic fourth-order tensor $\boldsymbol{C}^{\mathrm{Ani}}$ is given by:

$$\boldsymbol{C}^{\mathrm{Iso}} = 3\kappa_t \boldsymbol{I}^{\mathrm{vol}} + 2\mu_t \boldsymbol{I}^{\mathrm{dev}}, \tag{A.2}$$

where κ_t and μ_t depend on the chosen extraction method. Here, two methods are briefly recalled.

The *general method* (see Bornert et al., 2001) may be applied to any fourth-order tensor, even if it does not represent stiffness moduli. The isotropic part $\boldsymbol{C}^{\mathrm{Iso}}$ of $\boldsymbol{C}^{\mathrm{Ani}}$ is defined as follows:

$$\boldsymbol{C}^{\mathrm{Iso}} \equiv (\boldsymbol{I}^{\mathrm{vol}} :: \boldsymbol{C}^{\mathrm{Ani}})\boldsymbol{I}^{\mathrm{vol}} + \frac{1}{5}(\boldsymbol{I}^{\mathrm{dev}} :: \boldsymbol{C}^{\mathrm{Ani}})\boldsymbol{I}^{\mathrm{dev}}, \tag{A.3}$$

and the two scalars κ_t and μ_t are readily found as:

$$3\kappa_t = \boldsymbol{I}^{\mathrm{vol}} :: \boldsymbol{C}^{\mathrm{Ani}} \tag{A.4}$$

$$10\mu_t = \boldsymbol{I}^{\mathrm{dev}} :: \boldsymbol{C}^{\mathrm{Ani}}. \tag{A.5}$$

The second method applies to fourth-order tensors representing material tangent operators. It further requires that the tangent operator may be written according to the following *spectral* decomposition proposed by Ponte Castañeda (1996):

$$\boldsymbol{C}^{\mathrm{Ani}} = 3k_1 \boldsymbol{I}^{\mathrm{vol}} + 2k_2\left(\boldsymbol{I}^{\mathrm{dev}} - \frac{2}{3}\boldsymbol{N}\otimes\boldsymbol{N}\right) + 2k_3\left(\frac{2}{3}\boldsymbol{N}\otimes\boldsymbol{N}\right), \tag{A.6}$$

where $\boldsymbol{N}$ is typically normal to a yield surface in stress space and satisfies:

$$N_{ij} = N_{ji}, \quad N_{mm} = 0, \quad \boldsymbol{N} : \boldsymbol{N} = \frac{3}{2}. \tag{A.7}$$

The method relies on the assumption that the strain rate $\dot{\boldsymbol{\varepsilon}}$ is collinear with $\boldsymbol{N}$. Hence, the incremental relation $\Delta\boldsymbol{\sigma} \simeq \boldsymbol{C}^{\mathrm{Ani}} : \Delta\boldsymbol{\varepsilon}$ reduces to $\Delta\boldsymbol{\sigma} \simeq \boldsymbol{C}^{\mathrm{Iso}} : \Delta\boldsymbol{\varepsilon}$, where $\boldsymbol{C}^{\mathrm{Iso}}$ is the isotropic part of $\boldsymbol{C}^{\mathrm{Ani}}$ and is defined as:

$$\kappa_t = k_1, \quad \mu_t = k_3. \tag{A.8}$$

A.2. Extraction of transversely isotropic part of anistropic tensors

The projection method described here for extracting the transversely isotropic part of any fourth-order tensor was first proposed by Walpole (1981). First observe that any transversely isotropic second-order tensor $\boldsymbol{c}$ can be written as a combination of two basis tensors $\boldsymbol{a}$ and $\boldsymbol{b}$:

$$\boldsymbol{c} = \alpha\boldsymbol{a} + \beta\boldsymbol{b}, \tag{A.9}$$

where

$$\boldsymbol{a} = \boldsymbol{w}\otimes\boldsymbol{w}, \quad \boldsymbol{b} = \boldsymbol{1} - \boldsymbol{a}, \tag{A.10}$$

$\boldsymbol{w}$ being the direction of anisotropy and $\|\boldsymbol{w}\| = 1$.

The general fourth-order tensor $\boldsymbol{T}$ for transverse isotropy may be constructed as an arbitrary linear combination of six elementary tensors as:

$$\boldsymbol{T} = \sum_{i=1}^{6} T_i \boldsymbol{E}_i, \tag{A.11}$$

where the six basis tensors $\boldsymbol{E}_i$ are constructed from $\boldsymbol{a}$ and $\boldsymbol{b}$ as:

$$(E_1)_{ijkl} = \frac{1}{2} b_{ij} b_{kl} \tag{A.12}$$

$$(E_2)_{ijkl} = a_{ij} a_{kl} \tag{A.13}$$

$$(E_3)_{ijkl} = \frac{1}{2}(b_{ik}b_{jl} + b_{jk}b_{il} - b_{ij}b_{kl}) \tag{A.14}$$

$$(E_4)_{ijkl} = \frac{1}{2}(b_{ik}a_{jl} + b_{il}a_{jk} + b_{jl}a_{ik} + b_{jk}a_{il}) \tag{A.15}$$

$$(E_5)_{ijkl} = a_{ij} b_{kl} \tag{A.16}$$

$$(E_6)_{ijkl} = b_{ij} a_{kl} \tag{A.17}$$

The six coefficients T_i are given by (see Pierard and Doghri, 2006b):

$$\begin{aligned} T_1 &= \boldsymbol{E}_1 :: \boldsymbol{T}, \quad T_2 = \boldsymbol{E}_2 :: \boldsymbol{T}, \\ T_3 &= \frac{1}{2}\boldsymbol{E}_3 :: \boldsymbol{T}, \quad T_4 = \frac{1}{2}\boldsymbol{E}_4 :: \boldsymbol{T}, \\ T_5 &= \frac{1}{2}\boldsymbol{E}_6 :: \boldsymbol{T}, \quad T_6 = \frac{1}{2}\boldsymbol{E}_5 :: \boldsymbol{T}. \end{aligned} \tag{A.18}$$

The transversely isotropic tensor $\boldsymbol{T}$ may be rewritten in the following symbolic form:

$$\boldsymbol{T}^{\mathrm{TrIso}} = (T_1, T_2, T_3, T_4, T_5, T_6). \tag{A.19}$$

For the particular case of $\boldsymbol{w}$ aligned with direction 1, the 6 coefficients are related to components as:

$$T_1 = T_{2222} + T_{2233}, \quad T_2 = T_{1111}$$
$$T_3 = T_{2222} - T_{2233}, \quad T_4 = 2T_{1212} \tag{A.20}$$
$$T_5 = T_{1133}, \quad T_6 = T_{3311}$$

Let us now consider any anisotropic fourth-order tensor $\boldsymbol{T}^{Ani}$. Application of the double contractions in (A.18) on $\boldsymbol{T}^{\mathrm{Ani}}$ gives the projection of $\boldsymbol{T}^{\mathrm{Ani}}$ onto the subspace generated by $\boldsymbol{E}_i$ and yields a transversely isotropic tensor with direction of anisotropy $\boldsymbol{w}$:

$$\boldsymbol{T}^{\mathrm{TrIso}} = (\boldsymbol{E}_1 :: \boldsymbol{T}^{\mathrm{Ani}})\boldsymbol{E}_1 + (\boldsymbol{B}_2 :: \boldsymbol{T}^{\mathrm{Ani}})\boldsymbol{E}_2 + \frac{1}{2}(\boldsymbol{E}_3 :: \boldsymbol{C}^{\mathrm{Ani}})\boldsymbol{E}_3 \tag{A.21}$$
$$+ \frac{1}{2}(\boldsymbol{E}_4 :: \boldsymbol{T}^{\mathrm{Ani}})\boldsymbol{E}_4 + \frac{1}{2}(\boldsymbol{E}_6 :: \boldsymbol{T}^{\mathrm{Ani}})\boldsymbol{E}_5 + \frac{1}{2}(\boldsymbol{E}_5 :: \boldsymbol{T}^{\mathrm{Ani}})\boldsymbol{E}_6. \tag{A.22}$$

Appendix B. Reference tangent operators in incremental mean-field schemes

B.1. Incremental Mori-Tanaka scheme

In the M-T incremental scheme of Pierard and Doghri (2006b), the reference operator is defined as the isotropic part of the algorithmic J_2 tangent operator $\boldsymbol{C}^{\mathrm{alg}}$ according to the spectral isotropisation method (Appendix A.1). This isotropic extraction softens $\boldsymbol{C}^{\mathrm{alg}}$ in a direction orthogonal to $\boldsymbol{N}$ (Chaboche et al., 2005). The isotropic operator writes:

$$\widehat{\boldsymbol{C}}^{\mathrm{Iso,spe}} = 3\kappa^{\mathrm{el}}\boldsymbol{I}^{\mathrm{vol}} + 2\mu^{\mathrm{Iso,spe}}\boldsymbol{I}^{\mathrm{dev}}, \tag{B.1}$$

with

$$\mu^{\mathrm{Iso,spe}} = \mu_0\left(1 - \frac{3\mu_0}{h}\right). \tag{B.2}$$

where μ_0 is the elastic shear modulus of the matrix and $h = 3\mu_0 + \frac{d\sigma_y}{dp}$.

In the original method proposed by Doghri and Ouaar (2003), $\widehat{\boldsymbol{C}}^{\mathrm{Iso,spe}}$ is only used for computing Eshelby's tensor. The anisotropic algorithmic operator is used for other occurrences of $\widehat{\boldsymbol{C}}_0$ in Eq. (16). However, the study conducted by Pierard and Doghri (2006b) showed that it was desirable to compute Eshelby's tensor $\boldsymbol{S}$ and Hill's tensor $\boldsymbol{P} \equiv (\boldsymbol{S} : \widehat{\boldsymbol{C}}_0^{-1})$ with the same tensor in order to avoid unphysical results in some cases. Moreover, they showed that using $\widehat{\boldsymbol{C}}^{\mathrm{Iso,spe}}$ in all occurrences of $\widehat{\boldsymbol{C}}_0$ gives good results as well. For simplicity, only this combination will be considered in this work.

The approach was used to model the macroscopic behavior of elasto-plastic composites reinforced by spherical (Doghri and Ouaar, 2003) and ellipsoidal (Pierard et al., 2007) inclusions, and provides very good predictions of the macroscopic response in many cases. However, it was shown by Delannay et al. (2007) that the method underestimates the inclusion response when applied to two-phase steel.

B.2. Modified incremental Mori-Tanaka scheme

In order to improve the inclusion response of the incremental M-T scheme, Delannay et al. (2007) proposed a modified scheme which is able to raise the stress level in the inclusion. The method relies on a heuristic correction of the shear modulus of the matrix reference tangent operator. The latter is defined as intermediate between the elastic shear modulus and the shear modulus given by the spectral isotropisation method:

$$\mu^{\mathrm{heur}} = V\mu^{\mathrm{el}} + (1 - V)\mu^{\mathrm{Iso,spe}} \tag{B.3}$$

where:

$$V = \exp\left(-A_0\left(1 - \frac{c_1}{V_{\max}}\right)\left(\frac{\sigma_{eq}^I}{\sigma_{eq}^M} - 1\right)\right) \quad \text{if} \quad \sigma_{eq}^I > \sigma_{eq}^M \tag{B.4}$$

$$V = 1 \quad \text{if} \quad \sigma_{eq}^I \leqslant \sigma_{eq}^M. \tag{B.5}$$

In Eqs. (B.4) and (B.5), σ_{eq}^I and σ_{eq}^M are the average equivalent stress of the inclusion and matrix, respectively, c_1 is the inclusion volume fraction and $V_{\max}$ and A_0 are fitting parameters. Delannay et al. (2007) initially designed this model for simulating two-phase steel under cyclic loading, taking $A_0 = 7.5$ and $V_{max} = 0.53$. In this case, the method improves significantly the inclusion response, leading to accurate predictions of the macroscopic as well as phase responses. However, the method suffers from a lack of theoretical justification, and is a priori not predictive for other composite materials.

References

ABAQUS, 2007. General-Purpose Finite Element Software. ABAQUS Inc., Pawtucket, RI, USA.

Benveniste, Y., 1987. A new approach to the application of Mori-Tanaka's theory in composite materials. Mech. Mater. 6, 147–157.

Benveniste, Y., Dvorak, G.J., Chen, T., 1991. On diagonal and elastic symmetry of the approximate effective stiffness tensor of heterogeneous media. J. Mech. Phys. Solids 39, 927–946.

Berveiller, M., Zaoui, A., 1979. An extension of the self-consistent scheme to plastically-flowing polycrystals. J. Mech. Phys. Solids 26, 325–344.

Bornert, M., Bretheu, T., Gilormini, P., 2001. Homogénéisation en mécanique des matériaux. Hermes Science, Paris.

Brassart, L., Inglis, H.M., Delannay, L., Doghri, I., Geubelle, P.H., 2009. An extended Mori-Tanaka homogenization scheme for finite strain modeling of debonding in particle-reinforced elastomers. Comp. Mater. Sci. 45, 611–616.

Chaboche, J.L., Kanouté, P., Roos, A., 2005. On the capabilities of mean-field approaches for the description of plasticity in metal matrix composites. Int. J. Plasticity 21, 1409–1434.

Corbin, S., Wilkinson, D., Embury, J., 1996. The bauschinger effect in a particulate reinforced Al alloy. Mater. Sci. Eng. A 207, 1–11.

Delannay, L., Doghri, I., Pierard, O., 2007. Prediction of tension-compression cycles in multiphase steel using a modified incremental mean-field model. Int. J. Solids Struct. 44, 7291–7306.

Delannay, L., Pierman, A.-P., Jacques, P., 2009. Assessment of a micro–macro modeling of the bending and unbending of multiphase steel sheets. Adv. Eng. Mater. 11, 148–152.

Doghri, I., Ouaar, A., 2003. Homogenization of two-phase elasto-plastic composite materials and structures: study of tangent operators, cyclic plasticity and numerical algorithms. Int. J. Solids Struct. 40, 1681–1712.

Eshelby, J.D., 1957. The determination of the elastic field of an ellipsoidal inclusion, and related problems. Proc. R. Soc. London A 241, 376–396.

Gilormini, P., 1995. Insuffisance de l'extension classique du modéle auto-cohérent au comportement non linéaire. C.R. Acad. Sci. Paris 320 (Série IIb), 115–122.

Guillemer-Neel, C., Bobet, V., Clavel, M., 1999. Cyclic deformation behaviour and bauschinger effect in ductile cast iron. Mater. Sci. Eng. A 272, 431–442.

Han, W., Eckschlager, A., Böhm, H.J., 2001. The effects of three-dimensional multi-particle arrangements on the mechanical behavior and damage initiation of particle-reinforced MMCs. Compos. Sci. Technol. 61, 1581–1590.

Hazanov, S., Huet, C., 1994. Order relationships for boundary condition effects in heterogeneous bodies smaller than the representative volume. J. Mech. Phys. Solids 42, 1995–2011.

Hershey, A.V., 1954. The elasticity of an isotropic aggregate of anisotropic cubic crystals. J. Appl. Mech. 21, 236–240.

Hill, R., 1965. Continuum micro-mechanics of elastoplastic polycrystals. J. Mech. Phys. Solids 13, 89–101.

Kröner, E., 1958. Berechnung der elastischen konstanten des vielkristalls aus den konstanten des einkristalls. Z. Physik 151, 504–518.

LLorca, J., Segurado, J., 2004. Three-dimensional multiparticle cell simulations of deformation and damage in sphere-reinforced composites. Mater. Sci. Eng. A 365, 267–274.

Masson, R., Zaoui, A., 1999. Self-consistent estimates for the rate-dependent elastoplastic behaviour of polycrystalline materials. J. Mech. Phys. Solids 47, 1543–1568.

Mori, T., Tanaka, K., 1973. Average stress in matrix and average elastic energy of materials with misfitting inclusions. Acta Metall. 21, 571–574.

NETGEN, 2004. Automatic Mesh Generator, Version 4.4. Available from <http://www.hpfem.jku.at/netgen>. J. Schöberl, University of Linz, Austria.

Pierard, O., Doghri, I., 2006a. An enhanced affine formulation and the corresponding numerical algorithms for the mean-field homogenization of elasto-viscoplastic composites. Int. J. Plasticity 22, 131–157.

Pierard, O., Doghri, I., 2006b. Study of various estimates of the macroscopic tangent operator in the incremental homogenization of elastoplastic composites. Int. J. Multiscale Comp. Eng. 4, 521–543.

Pierard, O., Gonzalez, C., Segurado, J., LLorca, J., Doghri, I., 2007. Micromechanics of elasto-plastic materials reinforced with ellipsoidal inclusions. Int. J. Solids Struct. 44, 6945–6962.

Ponte Castañeda, P., 1996. Exact second-order estimates for the effective mechanical properties of nonlinear composite materials. J. Mech. Phys. Solids 44, 827–862.

Ponte Castañeda, P., 2002. Second-order homogenization estimates for nonlinear composites incorporating field fluctuations: I-theory. J. Mech. Phys. Solids 50, 737–757.

Qiu, Y.P., Weng, G.J., 1990. On the application of Mori-Tanaka's theory involving transversely isotropic spheroidal inclusions. Int. J. Eng. Sci. 28, 1121–1137.

Rekik, A., Auslender, F., Bornert, M., Zaoui, A., 2007. Objective evaluation of linearization procedures in nonlinear homogenization: a methodology and some implications on the accuracy of micromechanical schemes. Int. J. Solids Struct. 44, 3468–3496.

Segurado, J., LLorca, J., 2006. Computational micromechanics of composites: the effect of particle spatial distribution. Mech. Mater. 38, 873–883.

Segurado, J., LLorca, J., González, C., 2002. On the accuracy of mean-field approaches to simulate the plastic deformation of composites. Scripta Mater. 46, 525–529.

Suquet, P., 1995. Overall properties of nonlinear composites: a modified secant moduli theory and its link with Ponte Castañeda's nonlinear variational procedure. C.R. Acad. Sci. Paris 320 (Série IIb), 563–571.

Tandon, G.P., Weng, G.J., 1988. A theory of particle-reinforced plasticity. J. Appl. Mech. 55, 126–135.

Walpole, L.J., 1981. Elastic behavior of composite materials: theoretical foundations. Adv. Appl. Mech. 21, 169–242.

Weissenbek, E., Böhm, H., Rammerstorfer, F., 1994. Micromechanical investigations of arrangement effects in particle reinforced metal matrix composites. Comp. Mater. Sci. 3, 263–278.